07 Apr 1995, 10:30 am - 11:30 am

Observed Surface Breakage due to Strike-Slip Faulting

C. A. Lazarte
University of California, Berkeley, California

J. D. Bray
University of California, Berkeley, California

Proceedings: Third International Conference on Recent Advances in Geotechnical Earthquake Engineering and Soil Dynamics, April 2-7, 1995, Volume II, St. Louis, Missouri

Observed Surface Breakage due to Strike-Slip Faulting

Paper No. 9.10

C.A. Lazarte and J.D. Bray
Department of Civil Engineering, University of California, Berkeley, California

SYNOPSIS: This paper presents observations from field studies and physical model tests to investigate the response of soil deposits to strike-slip bedrock faulting. The study is relevant to developing mitigation techniques against fault-induced damage in structures located near potentially active faults. Observations of ground rupture patterns in alluvial materials following the 1992 Landers earthquake are presented. Particularly important are the observations of significant deformation away from the main trace, the width of the shear zone, and the effects of the surficial geology on the fault expression. Preliminary results from small-scale model tests simulating strike-slip rupture are also presented. The tests results confirm that the width of the shear zone depends primarily on the ductility and height of the soil deposit. These studies provide insight regarding ground deformation patterns in the soil overlying strike-slip faulting.

INTRODUCTION

When a bedrock fault ruptures during an earthquake and propagates through overlying soil deposits up to or near the surface, where most constructed facilities are located, the damage due to fault rupture can be significant. Moreover, the damage can be catastrophic if the affected structure is a critical facility, such as a dam. Given that it is not feasible to stop a bedrock fault from rupturing, engineers should develop techniques to minimize the damaging effects of surface faulting. However, few techniques have been identified as effective strategies to mitigate such effects, other than the avoidance of construction near the recognized trace of a potentially active fault. Avoidance is not a panacea as some facilities (e.g., lifelines) cannot be sited to avoid crossing active faults and our ability to delineate all potential fault rupture zones is imperfect (e.g., 1992 Landers earthquake).

In order to develop techniques to minimize the impact of ground rupturing on structures near an active fault, it is necessary to identify the controlling factors in the phenomenon. The principal factors affecting surface faulting are: 1) the type of fault movement (normal, reverse, or strike-slip), 2) the inclination of the fault plane, 3) the amount of displacement on the fault, 4) the depth and geometry of the overlying earth materials, and 5) the characteristics of the overlying earth materials (e.g., Taylor and Cluff, 1977; Bonilla, 1988). Additionally, it is important to understand the kinematics and mechanisms involved in any particular type of faulting.

Although there has been great improvement in our understanding of the mechanisms of faulting on a tectonic scale, several questions remain regarding fault rupture propagation in soils. For example, it is important to identify the field of displacements and thus the field of deformation on the ground surface in the vicinity the fault breakage. An ensuing question is how the pattern observed on the surface reflects that which has developed in the bedrock and overlying soil.

The effect that different surficial materials sheared by the fault have on the deformation pattern should not be overlooked. The inherent deformability of soils ensures that some fraction of the total offset across a distinct base rock fault (occurring in a very narrow zone) will be distributed across a relatively larger mass of overlying deformed soil, and hence the distinct offset at the ground surface will be less than that at the bedrock-soil contact (Bray et al., 1994).

An early interpretation of the resulting patterns of surface deformation during a strike-slip fault movement and its relation to the different materials being sheared was rendered by Reid (1910) after the 1906 San Francisco earthquake (Figure 1).

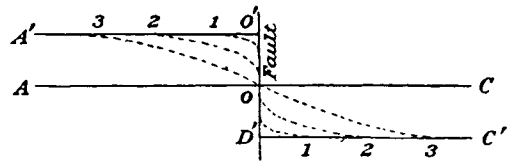

Fig. 1: Schematic plan view of deformation with depth in alluvium after strike-slip rupture (after Reid, 1910).

Originally straight, horizontal lines at various depths in the alluvium deposit have different positions after the bedrock fault ruptures. Line AOC on the bedrock (bottom of soil deposit) becomes A'O'D'C' without any offset absorption; line AOC on the ground surface now becomes A'3O3C' with all the bedrock fault offset absorbed as ground warping; whereas other lines at intermediate depths take intermediate positions. Although Reid gave an incisive description of the problem, even today, the underlying mechanisms are not yet fully understood nor the controlling parameters adequately quantified.

The primary source of information to unveil the mechanisms involved in this phenomenon should be the analysis of field data, which should be complemented with analytical and experimental techniques such as physical modeling. This paper presents field observations made following the 1992 Landers, California earthquake, which displayed a predominant strike-slip style of ground rupturing. Some comparisons are made with these field data and the results from some physical model tests as an attempt to enhance our understanding of faulting through soils and to set some basis for the development of ground rupture mitigation techniques.

FIELD STUDY: THE 1992 LANDERS EARTHQUAKE

Overview

The 28 June 1992 M_w = 7.3 Landers earthquake presented an excellent opportunity to study strike-slip faulting. The Landers event proved to be a valuable case history for a fortuitous combination of factors: the extensive length of rupture (more than 85 km), the very low population density of the area where the earthquake occurred (consequently, there was little obstruction due to buildings or other structures), and the arid climate and scarce vegetation, which helped express the numerous surface ruptures unusually well for considerable time. During the Landers earthquake sequence at least five faults were ruptured (Figure 2).

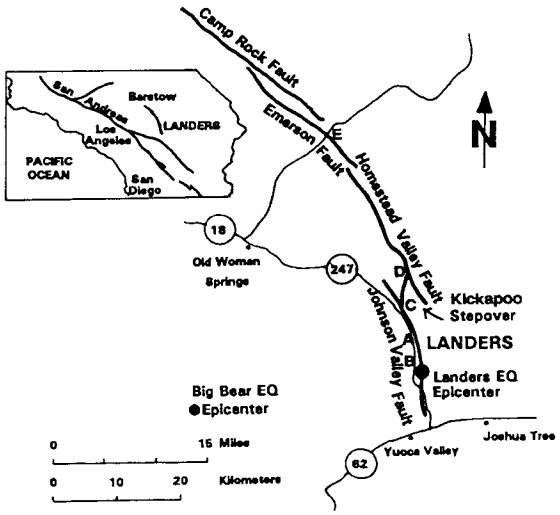

Fig. 2: The principal faults activated by the 1992 Landers earthquake.

The shallow (less than 10-km deep) focal mechanism was mainly strike-slip, which produced up to 6 m of right-lateral displacement (typically 2 to 3 m). Although the overall movement was primarily right-lateral, some sections of the rupture exhibited up to 1.5 m of vertical displacement, while some short strands (possibly kinematically related to the predominant, longer traces) ruptured left-laterally.

The Landers earthquake rupture area lies in a region of linear, northwest trending mountain range with wide alluvial basins between them. The thicknesses of unconsolidated deposits ranges from a few meters, in the margins of the basins, up to around 100 m across the valleys, according to well boring logs. Often, weathered, rocky knobs protrude in the mildly sloping, alluvial valleys. The principal components of bedrock in the rupture area are granitic (the prevalent type) and metamorphic rocks (only in a few outcrops). In general terms, the quaternary geology is complex, and includes Holocene to late Pleistocene alluvial deposits consisting of fan, wash, terrace, and eolian units (Sowers et al., 1994). Typically, the surficial alluvial deposits are formed of granitic, coarse-to-medium sand and fine gravel with less than 20% of non-plastic fines. The rupture also affected two small, flat areas (playas) containing finer grained materials. Thus, the types of earth materials ruptured were mostly weathered bedrock and stiff (often cemented) alluvium (Fenton and Bray, 1994).

Description of surface breakage

A salient feature of the surface breakage during the Landers earthquake was that, along much of the rupture length, the fault zones were broad shear zones rather than narrow, simple traces. In alluvial deposits, the surface breakage pattern indicates that the width of the shear zone, where potentially damaging levels of offset took place, can be considerable, up to hundreds of meters wide (Johnson et al., 1994; Lazarte et al., 1994; Lajoie, 1994). These broad shear zones were expressed as multiple, approximately parallel, closely-spaced strands. Typically, one of the strands, the main trace, concentrated much of the total right-lateral offset observed across the entire shear zone; one or two additional, noticeable strands then accounted for much of the remaining offset; and lastly, numerous other closely-spaced cracks accommodated the rest of the total offset. Where the conspicuous strands were about less than 10 meters apart, the ground between them was intensively distorted, cracked, and, in many instances, completely shattered. Often, gravity grabens developed between the bounding strands. Where the main strands were more distant, up to hundreds of meters apart, a tabular shear-zone was created (Johnson et al., 1994). This zone had numerous en-echelon tension cracks and left-lateral fractures trending obliquely to the bounding walls.

In the case of a single fault segment, the following offset patterns, with three levels of fracturing, can be recognized:

1) A high level of deformation, with offsets greater than 1 m, and on average up to 3 m, taking place in the immediate vicinity of the main trace, i.e., a zone about 10 m wide centered about the main trace.
2) An intermediate level, where individual fractures had offsets up to a few tenths of a meter, occurring in an area up to 100-m wide, and
3) A low level of deformation, characterized by extensional cracks with openings on the order of a few millimeters, observed in some localities up to 500 to 700 m away from the main trace.

Although the amount of slip varied along the rupture length (Hudnut and Larsen, 1993), and thus the magnitudes of offset in the above categories should be adjusted accordingly, the described pattern of decreasing magnitude was consistent in the alluvial deposits.

In addition to the concentrated offset along fractures, ground surface distortion, or simple shear deformation, took place between adjacent fractures with the same trend of decreasing magnitude at greater distances from the main rupture. Both offset along individual fractures and deformation due to ground distortion accounted for the total relative displacements in the broad shear zones. In the tabular shear zones, with two or more traces of intense and comparable level of shearing, one can interpret the resulting offset configuration as the superposition of two or more of the simple patterns described above. Examples of lateral distribution of ground deformation are shown in Figure 3.

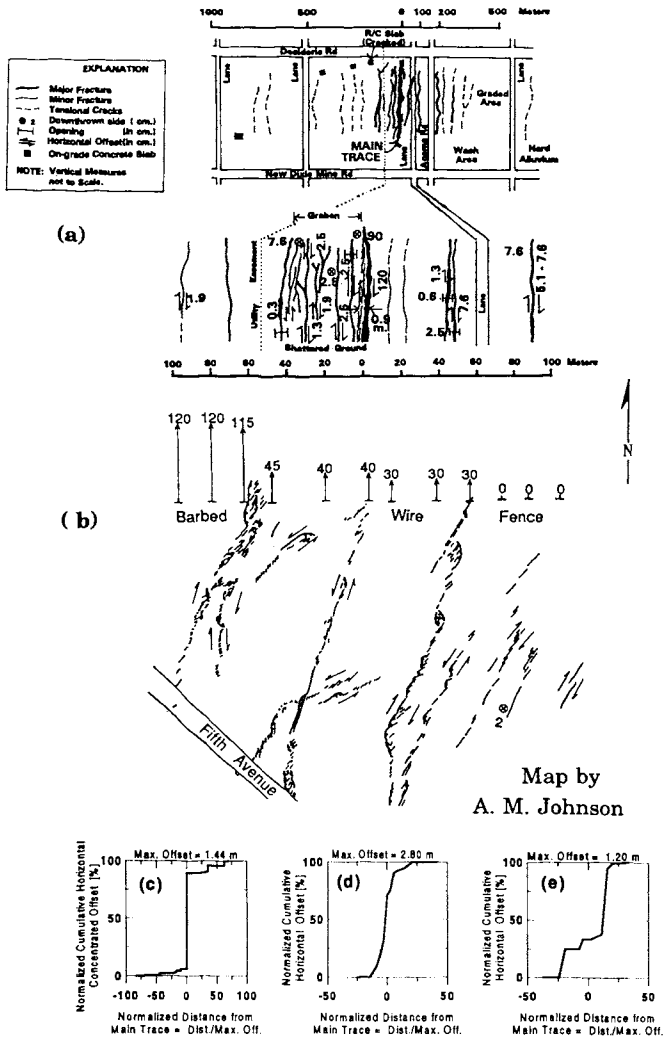

Fig. 3: Examples of patterns of deformation: **(a)** Concentrated right-lateral offset across the Johnson Valley Fault near Landers (Lazarte et al., 1994); **(b)** Relative displacements normal to a fenceline along the Kickapoo Fault near Fifth Av., North Landers (Lazarte et al., 1994); **(c)** Normalized cumulative concentrated right-lateral offset corresponding to diagram (a); **(d)**Normalized ground deformation as the Johnson Valley Fault crosses a fenceline on Encantado Rd., Landers (Lajoie, 1994); and **(e)** Cumulative offset corresponding to diagram(b).

Figure 3a depicts the offset distribution near the town of Landers, where the breakage was expressed as a main trace with multiple, subsidiary ruptures (Lazarte et al., 1994). Figure 3b shows how a fenceline was deformed by the Kickapoo fault (stepover area) near Landers (Lazarte et al., 1994). Here, both concentrated and distortional offsets are incorporated in the slip vectors. Figure 3c shows the distribution of the normalized cumulative concentrated offset as a function of distance from the main trace (normalized with respect to the maximum cumulative offset) corresponding to Figure 3a. Figure 3d shows the distribution of the normalized cumulative total displacement measured in a fenceline deformed by the rupture of the Johnson Valley fault at Landers (Lajoie, 1994). In Figure 3e, a more complex pattern corresponding to Figure 3b is presented. At this locality, the superposition of multiple simple patterns may account for the more spread out and complex distribution of offset observed across this shear zone.

Effect of Surficial Geology

The style of faulting, in general, and width of the rupture area, in particular, varied with the surficial geology along the breakage length, although other important factors (e.g. fault geometry, fault age, and the location of stepover zones often contributed to exceptions to this rule, especially at the regional scale; Fenton and Bray, 1994). A number of observations on a project scale (features approximately up to 100 m long), however, suggest that the rupture zone was narrower and more distinct (fewer fractures accommodating all the offset) in weathered bedrock. Conversely, in alluvial materials the rupture zone was more spread out and more diffuse (many more fractures with smaller offset, and commonly accompanied with distortion between adjacent fractures). An example of the changing surficial expression of a fault due to dissimilar materials is shown in Fig. 4, where the main trace of the Homestead Valley fault crossed two weathered bedrock outcrops and a sandy wash (Lazarte et al., 1994). The rupture zone in the alluvium was more than 5 m wide, whereas it was restricted to a narrow area not more than 0.5 m wide in the outcrops.

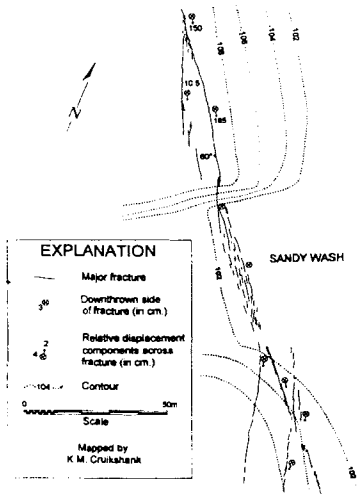

Fig. 4: Effects of surficial geology on the expression of the Homestead Valley Fault as it crossed an alluvial wash between weathered bedrock (after Lazarte et al., 1994).

Summary of Field Study

The observations of surface breakage at Landers suggest that fault zones can be considerably wide and often exhibit complex patterns in alluvial deposits. The magnitude of deformation is greatest along a zone around the main trace, and it progressively attenuates at increasing distance. Multiple, principal traces produce a pattern formed of more or less superimposed simple fault offset distributions. The surficial geology was an important factor in the expression and width of the faults. All of these observations should not be overlooked regarding siting facilities near a potentially active fault and developing ground rupture mitigation measures.

PHYSICAL MODELING

Testing Device

An experimental program with 1-g small-scale physical models is being carried out to better understand the process of strike-slip faulting in soils. The utilized testing machine, shown in Figure 5, simulates the horizontal movement of a vertical, strike-slip fault propagating in an overlying soil deposit.

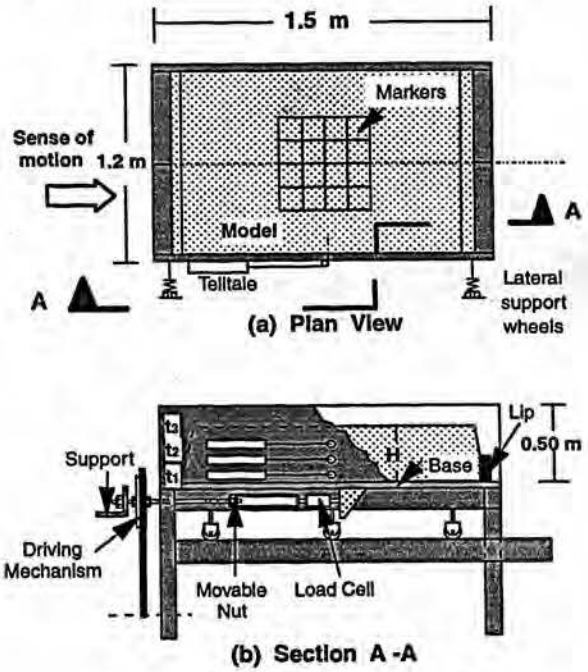

Fig. 5: Testing device.

The design allows flexibility in the geometry of the overlying soil (e.g., embankments and level ground) and various boundary constraints of the model, whose height can reach 0.5 m. The displacement-controlled driving system, which has a wide range of base displacement rates (from 4.3 to 700 mm/min), imparts horizontal motion to the split base on which the model is placed. A good grip between model and base is obtained through the use of expanded metal as a bedrock-soil interface. A load cell measures the total force applied to the movable half-base. The relative displacements within the model are measured by customized telltales (t1, t2, t3) and by surveying the position of embedded markers with the aid of image analysis. The base displacement is also measured and, along with other electronic measurements, is automatically recorded by a data acquisition system. The accuracy of the force and displacements measurements are approximately 5 N and 0.5 mm, respectively. Images (photographs and videos) were obtained and analyzed to accurately measure the deformation patterns on the surface of the model.

Model Material

The use of a mix consisting of kaolinite and bentonite (66% and 33% by dry weight, respectively) and water under 1-g acceleration has proved to be an effective means to study qualitatively the characteristics of fault rupture propagation in soils (Bray et al., 1993). After thorough and careful mixing of the components, the obtained saturated cohesive material was fairly homogeneous. Its water content was maintained at 115 ± 3%, approximately 25% below its liquid limit. The obtained consistency permits the mix to be placed easily and, more importantly, the fractures to be expressed satisfactorily. The low permeability of the mix and the relative short duration of the tests (between 9 and 240 sec.) restricts the model from consolidating while being loaded. The full-saturation condition, the absence of entrapped air, and the lack of consolidation during loading makes the model a nearly-incompressible material throughout the tests.

Changing the amount of water in the mix allows for varying mechanical properties, such as strength and strain at failure, in a controlled manner. It is particularly important to have control of the model material's failure strain because it represents a measure of the ductility of the material, and thus its ability to redistribute the base offset across a larger volume of material. Other factors that affect the undrained shear strength, S_u, and the strain at failure, ε_f, are the sitting time (time elapsed between remolding and testing) and the shearing rate. From examining Figure 6,

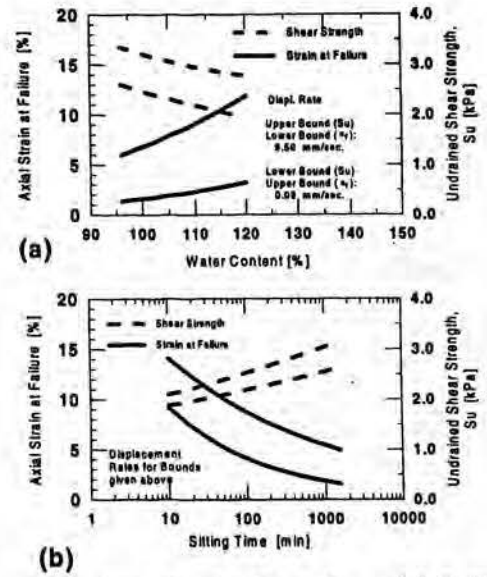

Fig. 6: Factors affecting S_u and ε_f. **(a)** Influence of water content; and **(b)** Effect of sitting time and displacement rate.

which presents the effects of water content, sitting time and shearing rate on S_u and ε_f in strain-controlled triaxial tests, it can be noticed that the mix exhibits moderate thixotropy. By using the same mix but with selective sitting times and under variable shearing rates, one can simulate materials with different levels of ductility.

Results

Preliminary tests on models 10 to 30 cm high simulating a prototype level soil deposit being sheared by a strike-slip fault were carried out. The base rupture propagates up into the model as the base starts moving and is observable at the bottom of the end faces. At early stages of the test, the top surface only warps, and elasto-plastic deformation takes place without cracking. The central portion of the model top surface (where end face effects are insignificant) exhibits a gradient of deformation across the model's width and an approximately constant deformation pattern longitudinally. Due to the boundary conditions, the gradient of deformation is zero at the model wall-clay interface and gradually increases up to a maximum at the centerline, where the pattern has its point of inflection, similar to that observed in the field (e.g., Fig. 3).

As the base displacement increases, the fractures initiated at the model base-clay interface grow upwards approximately in a mode III type of fracture. The originally vertical fault plane, striking parallel to the sense of motion at the bedrock, propagates upward as a complex, curved surface. In the central part of the model, the surface is essentially a vertical plane, whereas near the end faces it is curved. The degree of curvature can be controlled by varying the model height, front and rear lip height, and, to some extent, the material properties. At the end faces, the fracture tip also moves up, but off the centerline to allow for kinematics as observed in other fault configurations (i.e., dip-slip fault field studies and model experimentation show that the shear rupture is concave toward the downthown block, Bray et al., 1994). As the base displacement increases, the magnitude of distortion on the top surface also increases, although the general shape of the deformation pattern remains unchanged throughout the test before fracturing.

After a certain amount of base displacement, fractures appear on the surface, approximately in the center of the outer thirds of the length. The first cracks on the surface are disconnected segments, arranged en-echelon at a low inclination with the centerline. At later stages, the segmented fractures are connected in a single fracture that eventually severs the model. After a fracture appears on the surface, elasto-plastic deformation virtually ceases at that section, and the relative displacements between the two sides are essentially due to rigid-body motion, with relative movement concentrated along the existing shear crack. Typically, other secondary fractures subparallel to the main fracture are also observed. Fewer secondary cracks are observed when the material is relatively brittle.

Effect of Ductility on Fracture Expression

For a ductile material, the amount of base displacement to attain failure (fractures on the top surface) is larger compared to that needed for a more brittle material. This trend is shown in Figure 7, in which the normalized pattern of deformation on the surface of 30-cm high models for three levels of ductility is described. The pattern is plotted with respect to the distance from the centerline normalized to the base offset. For the same base displacement, a fracture on the surface has already appeared in the brittle model, and the elasto-plastic deformation essentially ceases prior to the present stage. As failure in the brittle model occurred at a smaller amount of base displacement, the pattern of distortion, which remains essentially "frozen" after cracking, is narrower in a brittle material.

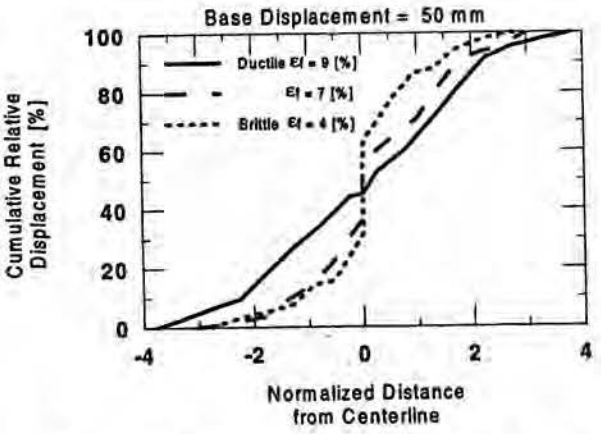

Fig. 7: Pattern of deformation in the models for different levels of ductility (For the same base displacement = 50 mm).

Conversely, for the same amount of base displacement, no fracture appears on the ductile model's surface, and elasto-plastic deformation is still occurring. Consequently, the extent of the deformed area will be broader. This trend in shear zone width as a function of material ductility is similar to what was observed at Landers and shown in Figure 4.

The ability of a soil deposit to absorb base deformation can be characterized by the offset absorption ratio (OAR) defined as the percentage ratio of the difference between the offsets at the base and the surface divided by the offset at the base. Before failure, OAR is 100%, whereas after failure its value depends on both the material ductility and the amount of base displacement. In the case of a perfectly rigid-brittle material, OAR is always zero because no base offset can be absorbed as deformation prior to failure, and the surface offset is identical to the base offset. In the brittle models, the magnitude of base offset that can be absorbed by elasto-plastic deformation before failure is relatively small, (or in other terms low OAR's) compared to that in ductile models. For the brittle model, at a base displacement of 50 mm, OAR = (18/50) x 100 = 36%. In the ductile model, for the same base displacement of 50 mm, OAR = 100%, as no fracture is on the surface. These observations may prove important in developing effective techniques to mitigate damage in areas overlying potentially active faults. For example, on the one hand, a ductile fill placed over a potentially active bedrock fault may be used to "locally absorb" the distinct base fault displacement and spread out the movement across a wider zone, thereby reducing differential settlement and extensional strains in this zone, but with the drawback of distorting a larger area.